PLOS ONE

RESEARCH ARTICLE

The bone is the major source of high circulating intact fibroblast growth factor-23 in acute murine polymicrobial sepsis induced by cecum ligation puncture

Jessica Bayer[1], Ravikumar Vaghela[1¤], Susanne Drechsler[2], Marcin F. Osuchowski[2], Reinhold G. Erben[1]*, Olena Andrukhova[1†]

1 Department of Biomedical Sciences, University of Veterinary Medicine Vienna, Vienna, Austria, **2** Ludwig Boltzmann Institute for Experimental and Clinical Traumatology in the AUVA Research Center, Vienna, Austria

† Deceased.
¤ Current address: Department of Plastic and Hand Surgery of Universitätsklinikum Erlangen, Erlangen, Germany
* Reinhold.Erben@vetmeduni.ac.at

Citation: Bayer J, Vaghela R, Drechsler S, Osuchowski MF, Erben RG, Andrukhova O (2021) The bone is the major source of high circulating intact fibroblast growth factor-23 in acute murine polymicrobial sepsis induced by cecum ligation puncture. PLoS ONE 16(5): e0251317. https://doi.org/10.1371/journal.pone.0251317

Editor: Partha Mukhopadhyay, National Institutes of Health, UNITED STATES

Received: August 13, 2020

Accepted: April 23, 2021

Published: May 14, 2021

Data Availability Statement: All relevant data are within the manuscript and its Supporting Information files.

Funding: This work was supported by a grant from the Austrian Science Fund (FWF P 26534-B13) to O.A. and R.G.E. The funders had no role in study design, data collection and analysis, decision to publish, or preparation of the manuscript.

Competing interests: The authors have declared that no competing interests exist.

Abstract

Fibroblast growth factor-23 (FGF23), a bone-produced hormone, plays a critical role in mineral homeostasis. Human diseases associated with excessive intact circulating FGF23 (iFGF23) result in hypophosphatemia and low vitamin D hormone in patients with normal kidney function. In addition, there is accumulating evidence linking FGF23 with inflammation. Based on these studies and the frequent observation of hypophosphatemia among septic patients, we sought to elucidate further the relationship between FGF23 and mineral homeostasis in a clinically relevant murine polymicrobial sepsis model. Medium-severity sepsis was induced by cecum ligation puncture (CLP) in adult CD-1 mice of both sexes. Healthy CD-1 mice (without CLP) were used as controls. Forty-eight hours post-CLP, spontaneous urine was collected, and serum, organs and bones were sampled at necropsy. Serum iFGF23 increased ~20-fold in CLP compared to control mice. FGF23 protein concentration was increased in the bones, but not in spleen or liver of CLP mice. Despite the ~20-fold iFGF23 increase, we did not observe any significant changes in mineral homeostasis or parathyroid hormone levels in the blood of CLP animals. Urinary excretion of phosphate, calcium, and sodium remained unchanged in male CLP mice, whereas female CLP mice exhibited lower urinary calcium excretion, relative to healthy controls. In line with renal FGF23 resistance, expression of phosphate-, calcium- and sodium-transporting proteins did not show consistent changes in the kidneys of male and female CLP mice. Renal expression of the co-receptor αKlotho was downregulated in female, but not in male CLP mice. In conclusion, our data demonstrate that the dramatic, sex-independent rise in serum iFGF23 post-CLP was mainly caused by an upregulation of FGF23 secretion in the bone. Surprisingly, the upsurge in circulating iFGF23 did not alter humoral mineral homeostasis in the acutely septic mice. Hence, the biological function of elevated FGF23 in sepsis remains unclear and warrants further studies.

Introduction

Fibroblast growth factor 23 (FGF23) is a 32 kDa glycoprotein mainly synthesized by osteoblast and osteocytes [1–4] in response to elevated serum phosphate [5–9], calcium [8], vitamin D [6,10,11] and parathyroid hormone (PTH) [12–16]. FGF23 is indispensable to maintain systemic mineral and vitamin D homeostasis. In renal proximal tubular epithelial cells, FGF23 controls phosphate reabsorption from the urine by downregulating the cell surface expression of the sodium-phosphate co-transporters type 2a (NaPi2a) and 2c (NaPi2c), thus augmenting renal phosphate excretion [17–21]. Furthermore, FGF23 suppresses 1α- hydroxylase (CYP27B1) [17] in proximal renal tubules, the key enzyme for producing the active vitamin D hormone $1,25(OH)_2D_3$ [22]. In distal renal tubules, FGF23 stimulates calcium reabsorption by increased trafficking of the epithelial calcium channel TRPV5 (transient receptor potential vanilloid-5) to the apical plasma membrane [23]. Moreover, FGF23 increases the membrane abundance of the sodium-chloride co-transporter NCC, one of the key molecules involved in Na^+-reabsorption in the kidney [24].

FGF23 signaling is mediated through the binding of the hormone to the ubiquitously expressed FGF receptors (FGFR). FGFR1c is considered to be the most important mediator of FGF23 effects [4,25]. However, FGFR3c and 4 may also be involved in FGF23 signaling in the kidney [26–28]. Under physiological conditions, the type 1 transmembrane protein αKlotho [29] serves as an essential co-receptor, allowing FGF23-mediated signal transduction by enhancing the binding of FGF23 to FGF receptors [25,30–32]. Proteolytic cleavage of full-length transmembrane Klotho produces the soluble isoform of Klotho (sKlotho) [33–35]. Recent evidence suggests that sKlotho, similar to transmembrane Klotho, functions as co-receptor for FGF23 signaling [32].

In addition to its regulatory effects on mineral homeostasis, recent studies have uncovered a new role of FGF23 in the systemic immune response. Several studies identified FGF23 as a potent stimulator of cytokine production in inflammatory cells such as macrophages, but also in hepatocytes [9,36,37]. Vice versa, inflammatory stimuli have been shown to elevate FGF23 expression and secretion from the osseous tissue [38–40]. In addition, increased *Fgf23* mRNA expression was also detected in extra osseous-tissues, especially in the spleen in lipopolysaccharide (LPS)-treated mice [36]. In the latter study, Masuda *et al.* identified activated dendritic cells and macrophages as source of the LPS-induced rise in splenic FGF23 expression. This observation was corroborated by Bansal *et al.* who also attributed the elevation of circulating Fgf23 in LPS-treated mice to an increase in splenic *Fgf23* transcription [41]. A clinical study in patients suffering from acute kidney injury (AKI) found a positive association between sepsis severity and FGF23 serum level, underlining the potentially important role of FG23 as a putative immune-regulatory molecule in sepsis [42].

Sepsis is a life-threatening organ dysfunction caused by a dysregulation in the host response to an infection [43]. Despite improvements in medical diagnostics and interventions, sepsis remains a leading cause of death in critically ill patients worldwide [44]. Despite a decline of in-hospital mortality during recent years, mortality rates persist at unacceptably high levels, ranging 25–30% in sepsis and up to 50% in septic shock [45]. Reliable, clinically relevant animal models are of crucial importance to study the heterogeneous and complex pathophysiology of sepsis.

In the current study, we used the cecal ligation puncture (CLP) procedure to investigate further the role of FGF23 in the pathophysiology of sepsis. CLP is considered the gold standard [46,47] in sepsis modeling since the resulting polymicrobial sepsis closely recapitulates the features of human abdominal sepsis [48,49]. Using this model, we analyzed circulating intact FGF23 (iFGF23), mineral homeostasis, as well as FGF23 production in the bone, spleen and

liver of male and female mice. While we found a dramatic increase in circulating iFGF23 in mice of both sexes after CLP, this change did not translate into major abnormalities of mineral homeostasis. Interestingly, FGF23 protein expression was upregulated in the bone, but not in the spleen and liver of septic mice.

Materials and methods

Animals

Three- to six-month-old wild-type CD-1 mice (Harlan) of both sexes were kept at 22–24˚C with a 12 h/12 h light/dark cycle. Mice were fed a normal mouse chow (Abbed Lab and Vet Service, Vienna, Austria) and had access to tap water *ad libitum*. All animal studies were approved by the Viennese (Austria) legislative committee and were performed in strict accordance with guidelines for animal care and welfare (Animal Use Proposal Permission no: 343130/2013/14).

Ethical statement

To ensure a comprehensive observation, all animals were checked by trained professionals (i.e. DVMs and/or trained personnel) to identify deteriorating animals and prevent them from suffering. All mice were monitored for clinical signs of illness and their status was evaluated using our modified mouse clinical assessment scoring system (M-CASS; relying on body temperature, fur appearance, posture, mobility, alertness, startle, and righting reflex). starting 12 h post-CLP [50]. Rectal temperature was monitored (Fluke Series II thermometer, Fluke USA) at least twice daily (or more often whenever a mouse deteriorated). Starting with CLP, all mice received continuous analgesic treatment (0.05 mg/kg buprenorphine, Bupaq®, Richter Pharma, Austria) every 6–8 h.

Sepsis model

Animals were subjected to polymicrobial sepsis using the CLP procedure. The surgery was performed under isoflurane anesthesia with perioperative buprenorphine (0.05 mg kg^{-1}) in 1 ml of Ringer's solution. In brief, the cecum was tightly ligated below the ileo-cecal valve and was perforated twice with a 17-gauge needle at its base and apex. This constitutes a mild-to-medium severity CLP as it produced an approximate mortality of 40% in 3-month-old females and 70% in 3-month-old males subjected to CLP as second hit after trauma [51]. In the current study, 23% of animals were euthanized prior to the planned study endpoint at 48h, because they met the criteria for humane endpoints based on the above-mentioned custom-developed scoring approach [50].

After repositioning of the cecum, the abdomen was closed with single button sutures and skin with Histoacryl® tissue adhesive (B. Braun, Aesculap, Germany). Animals received imipenem/cilastatin (25/25 mg kg^{-1}) in Ringer's solution starting at 2 h post-CLP. For three consecutive days, animals received an additional fluid resuscitation in combination with analgesic therapy (buprenorphine/imipenem/cilastatin) twice daily, all given subcutaneously.

For the initial time course experiment, 20 μL of blood was collected via facial vein puncture from each animal as previously described by Weixelbaumer *et al.* [52], 24 h before CLP (baseline), as well as 6 h, 24 h, and 48 h after CLP. All samples were immediately diluted 1:10 in PBS containing EDTA to prevent clotting. After centrifugation 180 μL of plasma was stored at −80˚C for further analysis.

At necropsy, 48 h post-CLP, approx. 1 ml of blood was collected from *vena cava* and animals were euthanized by cervical dislocation. Urine was taken directly from the bladder during

necropsy and stored at -80˚C. The blood was centrifuged, and serum was stored in -80˚C for subsequent analysis. Liver, spleen, kidney, and bones were collected during necropsy. Healthy CD-1 mice of both sexes without any surgery were used as controls.

Biochemical measurements

Serum creatinine, phosphorus, sodium, and calcium, as well as urinary phosphorus, sodium, and calcium were analyzed using a Cobas c111 analyzer (Roche, Mannheim, Germany). For the time course experiment, C-terminal FGF23 and iFGF23 in plasma (diluted 1:10) was measured by ELISA (Immutopics Inc., San Clemente California, USA). For the main experiment (48 h post-CLP), intact PTH and iFGF23 in serum (for iFGF23 diluted 1:3) were determined by ELISA (Immutopics Inc., San Clemente California, USA and Kainos Laboratories, Inc., Tokyo, Japan, respectively). Absorbance was read using an Enspire 2300 multilabel reader (PerkinElmer, Massachusetts, USA). In the time course experiment, the detection limit (6 pg/mL) of the iFGF23 assay (Immutopics Inc., San Clemente California, USA) was assigned to samples below the detectable range of the assay. Serum cytokine levels were assessed by using Milliplex ® MAP Mouse cytokine/chemokine magnetic Bead Panel Assay (Merck, Darmstadt, Germany) on a Bio-Plex 200 System (Bio Rad, Hercules, USA).

RNA isolation and quantitative RT-PCR

Snap-frozen kidneys were homogenized, and total RNA was extracted using the TRI Reagent solution (Applied Bio-systems, Thermo Fischer Scientific, Bedford, USA) and reverse transcribed into cDNA using the High Capacity cDNA Reverse Transcription Kit (Applied Biosystems, Thermo Fischer Scientific, Bedford, USA). Quantitative RT-PCR was performed on a qTOWER^3 84 (Analytic Jena, Jena, Germany) using EvaGreen HOT FIREPol® EvaGreen® qPCR Mix Plus (Solis BioDyne, Tartu, Estonia). A melting curve analysis was done for all assays. Primer sequences are available on request. Expression of target genes was normalized to the expression of the housekeeping genes *low density lipoprotein receptor-related protein associated protein* (*LRPAP1*) and *death-associated protein-3* (*DAP3*).

Total cell membrane isolation

Whole mouse kidneys were homogenized in 20 mM Tris (pH 7.4/HCl), 5 mM $MgCl_2$, 5 mM NaH_2PO_4, 1 mM ethylenediamine tetra-acetic acid (EDTA, pH 8.0/NaOH), 80 mM surcrose in the presence of protease inhibitors (cOmplete™ ULTRA Tablets, Mini, EDTA-free, EASYpack, Roche, Mannheim, Germany). After sonication, samples were centrifuged for 15 min at 4,000 g. Subsequently, supernatants were centrifuged for an additional 30 min at 16.000 g. Pellets were dissolved in RIPA lysis buffer (50 mM Tris, pH 7.4, 150 mM NaCl, 1 mM EDTA, 1% Triton X-100, 1% sodium deoxycholate, 0.1% SDS) and stored at -80˚C until use.

Extraction, measurement and normalization of FGF23 protein from tissue

Femora were harvested during necropsy and bone marrow was removed by brief centrifugation. Bones were snap-frozen in liquid nitrogen and kept at -80˚C until use. Bone protein was extracted as described previously [53]. In brief, bones were incubated overnight in 1.2 M HCl with moderate agitation at 4˚ C. Subsequently, bones were incubated for 72 h in 6 M guanidinium-HCl at 4˚C while shaking. The supernatant of the latest extraction fraction was precipitated with 100% EtOH, washed with 75% EtOH, and the protein pellet was resuspended in RIPA lysis buffer (50 mM Tris, pH 7.4, 150 mM NaCl, 1 mM EDTA, 1% Triton X-100, 1% sodium deoxycholate, 0.1% SDS).

At necropsy, the liver and spleen were harvested, shock-frozen in liquid nitrogen and stored at -80˚C until further analysis. Frozen organs were homogenized in RIPA lysis buffer, and used for analysis. All solutions for homogenizing and protein extraction were supplemented with protease inhibitors (cOmplete™ ULTRA Tablets, Mini, EDTA-free, EASYpack, Roche, Mannheim, Germany). Bone and soft tissue lysates were used to quantify intact FGF23 (iFGF23) protein levels with the help of an ELISA Kit (Kainos Laboratories, Inc., Tokyo, Japan). Prior experiments were conducted to verify the suitability of the lysates for ELISA measurements. To overcome the inhibitory effects of the buffer components, lysates were diluted with the ELISA Kit internal standard 1 (0 pg/ml iFGF23) before being used in the ELISA. The iFGF23 levels were normalized to the total protein amount of each sample which was determined using Pierce™ BCA Protein Assay Kit (Thermo Fischer Scientific, Waltham, USA).

Western blot

Total cell membrane protein samples were solubilized in Laemmli buffer and heated for 10 min at 97˚C. Forty μg of protein/well were electrophoretically separated on a 10% polyacrylamide gel, and transferred to a PVDF membrane (GE healthcare, Chicago, USA). Consistent protein transfer was confirmed by Ponceau S staining. The membranes were blocked with 5% (w/v) non-fat dried milk, and incubated with gentle agitation at 4˚C with the primary antibodies dissolved in 2% (w/v) bovine serum albumin (BSA, Sigma Aldrich/Merck KGaA, Darmstadt, Germany). As primary antibodies, we used monoclonal mouse anti-TRPV5 (1:1,000, sc-398345, Santa Cruz Biotechnology Inc., Dallas, USA), polyclonal sheep anti-NCC (1:2,000, produced in house by Dario R. Alessi, University of Dundee, Dundee, UK), monoclonal mouse anti-NaPi2a (1:1,000, NBP2-42216, Novus Biologicals, Centennial, USA), monoclonal rat anti-human Klotho (1:500, KO603, Transgenic Inc., Fukuoka-shi, Japan), monoclonal mouse anti-GAPDH (1:500, MAB374, Merck KGaA, Darmstadt, Germany), and monoclonal mouse anti-β-actin (1:5,000, A5441, Sigma Aldrich/Merck KGaA, Darmstadt, Germany). Membranes which served as negative controls for the secondary antibody were incubated with BSA instead of the primary antibody. After washing, membranes were treated with the horseradish peroxidase-linked secondary antibodies diluted in 2.5% (w/v) non-fat dried milk for 1 h at room temperature. Specific binding was visualized by the enhanced chemiluminescence (ECL) substrate (Bio Rad, Hercules, USA). Images were captured using the Chemi Doc-It 600 Image System (UVP/Analytik Jena AG, Jena, Germany). Intensity of the protein bands was quantified by using Image Quant 5.0 software (Molecular Dynamics). The expression levels were normalized to β-actin expression. Each sample was used on two independent gels/membranes to create two technical replicates. Results from both replicates were averaged for further data analysis.

Statistics

All data represent the mean ± standard deviation of the mean (SD). All data sets were tested for normality and distribution of variance prior to analysis. In the time course experiment, a mixed model approach with Geisser-Greenhouse correction was conducted followed by Tukey *post hoc* test to assess the differences in plasma concentrations of iFGF23, C-terminal FGF23, and the iFGF23/C-terminal FGF23 ratio versus baseline within each sex. In the main experiment, two-way analysis of variance (ANOVA) was used to assess the influence of sex and of CLP, as well as their two-way interactions. In data sets showing a significant CLP effect in two-way ANOVA, individual group comparisons (CLP vs. healthy control) were performed using Student's t-test with Welch correction. Statistical analyses were performed using Prism 7 and

Prism 8 (GraphPad Software, San Diego, USA) and SPSS Statistics 25 (IBM Corp., Armonk, NY). Values of $p < 0.05$ were considered statistically significant.

Results

Sepsis increases circulating cytokine levels in both sexes

To confirm a systemic inflammatory response in CLP animals, we first examined serum levels of the inflammatory cytokines/chemokines interleukin (IL)-1ß, IL-6, IL-10, tumor necrosis factor-α (TNF-α), and keratinocyte-derived chemokine/chemokine ligand-1 (KC/CXCL1) in control and CLP mice of both sexes (Table 1). As expected, CLP mice exhibited a robust release of inflammatory mediators; e.g., serum KC/CXCL1 was ~60-fold higher in male and female CLP mice, relative to healthy controls, 48 h post-CLP. All other pro-inflammatory cytokines also tended to be elevated but due to the high variance within the CLP groups these increases did not reach statistical significance.

Sepsis-induced elevation of serum intact FGF23 is associated with an upregulated FGF23 expression in the bone but not in other tissues

To determine the optimal time point for subsequent experiments, we first conducted a time course study evaluating the plasma concentrations of C-terminal and iFGF23 in mice of both sexes after CLP (Fig 1A and 1B). In both sexes, CLP induced a rapid and distinct increase in C-terminal FGF23 which was followed by a more delayed rise in iFG23 plasma levels. Within 6 h post-CLP, the ratio of intact to C-terminal FGF23 dropped by ~80–90% in mice of both sexes (Fig 1). Based on these data, we performed all subsequent experiments at the 48 h time point.

When we measured iFGF23 serum concentration using a different assay (Kainos) compared with Fig 1 (Immutopics) in samples that were less diluted, we found the serum iFGF23 level (Fig 2) ~20-fold upregulated in CLP mice of both sexes vs. healthy controls, 48 h after CLP.

Prior studies [9,36,41] identified the spleen, more specifically resident macrophages and dendritic cells, as the major FGF23 expression site after an inflammatory stimulus. Additionally, Masuda *et al.* reported an increased hepatic *Fgf23* expression 2 h after the injection of LPS in mice [36]. Furthermore, a clinical study with patients suffering from autosomal dominant polycystic kidney disease (ADPKD)—the most common cause of genetic CKD—showed a significantly elevated expression of hepatic FGF23, accompanied by increased circulating FGF23 [54]. To identify the major source of increased circulating FGF23 in our CLP model, we examined the abundance of intact FGF23 in spleen, liver, and bone (Fig 2). Due to the very low

Table 1. Inflammatory markers in the serum of control and CLP mice, 48 h post-CLP.

Parameter (pg/ml)	♀Control n = 4	♀CLP n = 12	♂Control n = 4	♂CLP n = 14	Two-way ANOVA		
					Sex	CLP	Int.
IL-1β	13.58 ± 5.12	17.39 ± 8.14	10.98 ± 4.87	27.39 + 15.48 *	ns	p = 0.038	ns
IL-6	6.51 ± 3.42	1943 ± 4333	3.96 ± 2.13	5905 ± 9251	ns	ns	ns
IL-10	6.62 ± 2.24	432.2 ± 873.6	9.77 ± 2.56	1247 ± 1885	ns	ns	ns
TNF-α	7.65 ± 2.72	34.6 ± 34.30	7.48 ± 3.00	124.9 ± 215.42	ns	ns	ns
KC/CXCL1	75.73 ± 53.92	5229 ± 7035*	114 ± 20.81	6893 ± 8636 *	ns	p = 0.047	ns

Data are means ± SD. IL, interleukin; KC, keratinocyte-derived chemokine; CXCL1, chemokine ligand-1; TNF, tumor necrosis factor; Int., interaction between sex and CLP.

*, P<0.05 vs. healthy controls within same sex, Student's t-test with Welch corrections.

https://doi.org/10.1371/journal.pone.0251317.t001

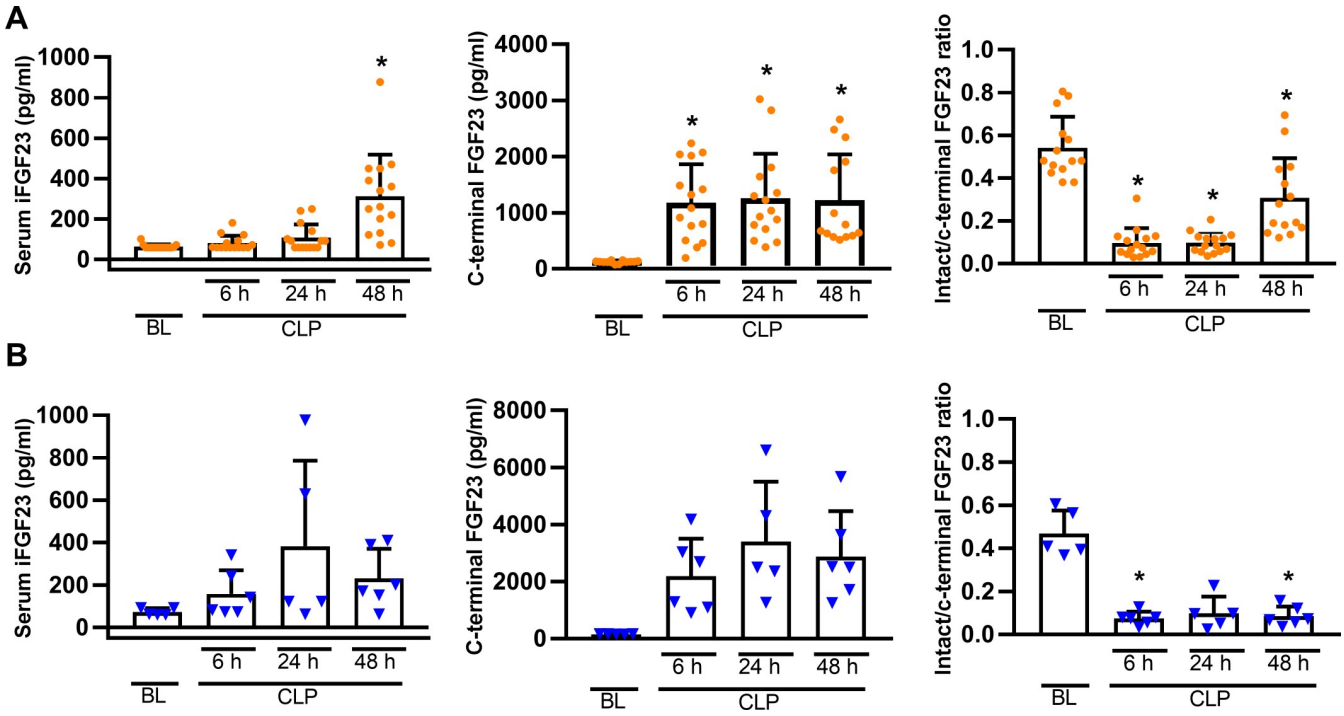

Fig 1. CLP-induced increase in plasma C-terminal and intact FGF23 levels. Plasma C-terminal and iFGF23 concentration in females (A) and males (B) increased post-CLP relative to baseline (BL; 24 h prior CLP). Each bar is the mean ± SD of 5–15 mice per group. Each symbol represents an individual sample. Mixed model approach with Geisser-Greenhouse correction, followed byTukey *post hoc test*.*, P<0.05 vs. baseline within same sex.

https://doi.org/10.1371/journal.pone.0251317.g001

abundance of FGF23 protein, we were unable to quantify splenic and hepatic FGF23 protein expression, using western blotting. Therefore, we measured splenic, hepatic and bone iFGF23 protein concentrations by ELISA (Fig 3).

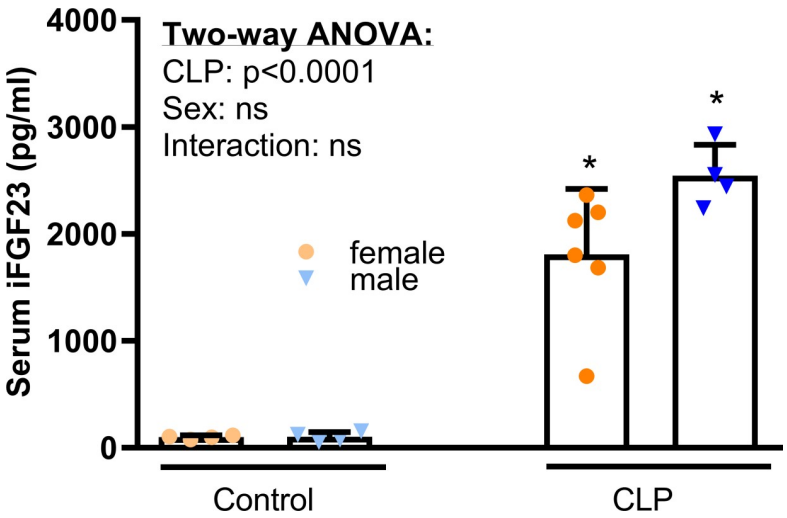

Fig 2. CLP-induced increase in serum iFGF23 levels, 48 h after surgery. Serum iFGF23 concentration increased profoundly in CLP mice of both sexes, relative to healthy controls. Each bar is the mean ± SD of 4–6 mice per group. Each symbol represents an individual sample. Inset shows results from two-way ANOVA. *, P<0.05 vs. healthy controls within same sex, Student's t-test with Welch corrections.

https://doi.org/10.1371/journal.pone.0251317.g002

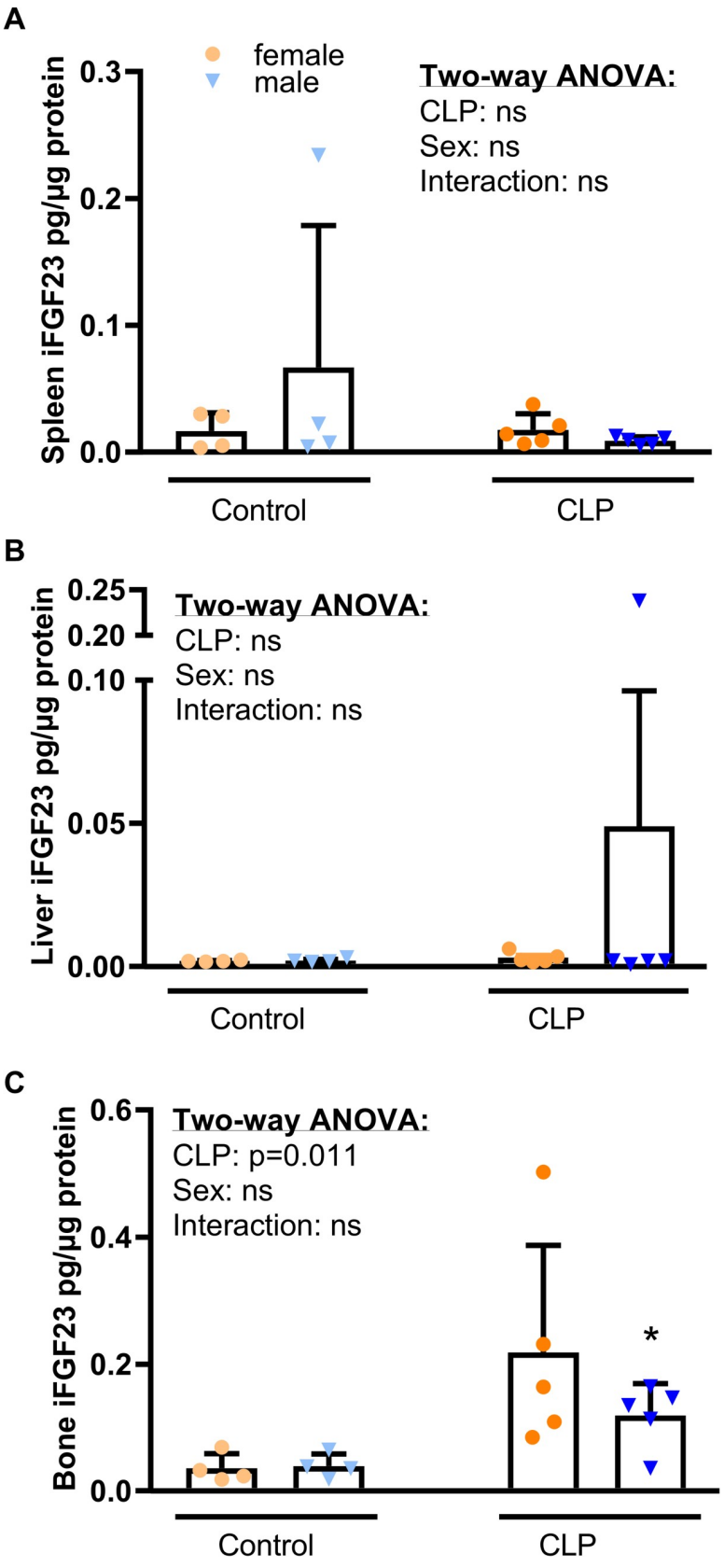
A
female
male
Two-way ANOVA:
CLP: ns
Sex: ns
Interaction: ns
Spleen iFGF23 pg/µg protein
0.3
0.2
0.1
0.0
Control
CLP
B
Two-way ANOVA:
CLP: ns
Sex: ns
Interaction: ns
Liver iFGF23 pg/µg protein
0.25
0.20
0.10
0.05
0.00
Control
CLP
C
Two-way ANOVA:
CLP: p=0.011
Sex: ns
Interaction: ns
Bone iFGF23 pg/µg protein
0.6
0.4
0.2
0.0
*
Control
CLP

Fig 3. iFGF23 protein expression in spleen, liver and bone after CLP. (A) Splenic, (B) hepatic and (C) bony iFGF23 protein expression measured in lysates from spleen, liver and bone by ELISA, 48 h post-surgery (n = 4–5 per group). Data are mean ± SD. Each symbol represents an individual sample. Insets show results from two-way ANOVA. *, $P < 0.05$ vs. healthy controls within same sex by Student's t-test with Welch correction.

https://doi.org/10.1371/journal.pone.0251317.g003

Interestingly, we did not observe significant differences in splenic (Fig 3A) and hepatic (Fig 3B) iFGF23 protein concentrations between control and CLP animals. In contrast, iFGF23 protein expression was markedly increased in the bones of CLP mice (Fig 3C). Hence, the bone appears to be the major source of increased circulating iFGF23 in CLP mice. Although FGF23 expression in the healthy kidney appears to be very low [17,55,56], increased renal FGF23 expression has been noted in several models of kidney disease [55,57,58]. Therefore, we quantified *Fgf23* mRNA expression in the kidney by qRT-PCR. However, *Fgf23* mRNA expression was undetectable in all groups of mice, showing that CLP does not upregulate *Fgf23* mRNA expression in the kidney (data not shown).

Circulating PTH and mineral homeostasis remain largely unchanged in septic mice

Several studies reported that PTH acts as a stimulator of skeletal FGF23 synthesis in rodents [12–16]. In addition, a transient increase of serum PTH has been reported after administration of LPS, heat-killed *Brucella abortus*, and IL-1β in mice [40,59]. We measured serum PTH to examine its potential role as a stimulator of FGF23 secretion in septic mice. However, we observed similar PTH levels in all groups (Fig 4A).

Sepsis frequently leads to single and/or multiorgan dysfunction [60], and the kidney is one of the organs which is affected at the earliest [61,62]. To evaluate kidney function, we analyzed serum creatinine level (Fig 4B). Consistent with a declining kidney function, we found increased serum creatinine in CLP mice of both sexes. This finding is in agreement with previous studies showing elevated circulating creatinine levels already 24 h after CLP [63–65]. Despite the profound changes in circulating FGF23, serum phosphate, sodium, and calcium concentrations remained unchanged in CLP mice (Fig 4C). Similarly, with the exception of reduced urinary calcium excretion in female CLP mice (baseline vs. CLP, $p = 0.056$), renal excretion of phosphate and sodium was comparable in control and CLP mice (Fig 4D).

Renal ion-transporting molecules are not regulated in a consistent manner in septic mice

To further explore the puzzling finding that mineral homeostasis remained largely unchanged in CLP mice despite a distinct elevation in circulating iFGF23, we investigated typical target molecules known to be regulated by FGF23 in the kidney. To this end, we isolated membrane fractions from kidney homogenates and quantified the abundance of mineral-transporting proteins by western blotting. In female CLP mice, renal expression of NaPi2a and NCC was similar to healthy controls, whereas the expression of TRPV5 and Klotho was reduced, 48 h post-CLP (Fig 5A). In male CLP mice, NaPi2a, NCC, TRPV5 and Klotho protein expression remained unchanged relative to control mice (Fig 5B).

FGF23 is known to regulate vitamin D metabolism in the kidney [17,56]. Therefore, we examined the mRNA expression of renal *1α-hydroxylase* (Fig 6). In female CLP mice, renal *1α-hydroxylase* remained unchanged, relative to controls. Although male CLP mice tended to have higher expression of renal *1α-hydroxylase* than healthy controls, this difference did not reach statistical significance.

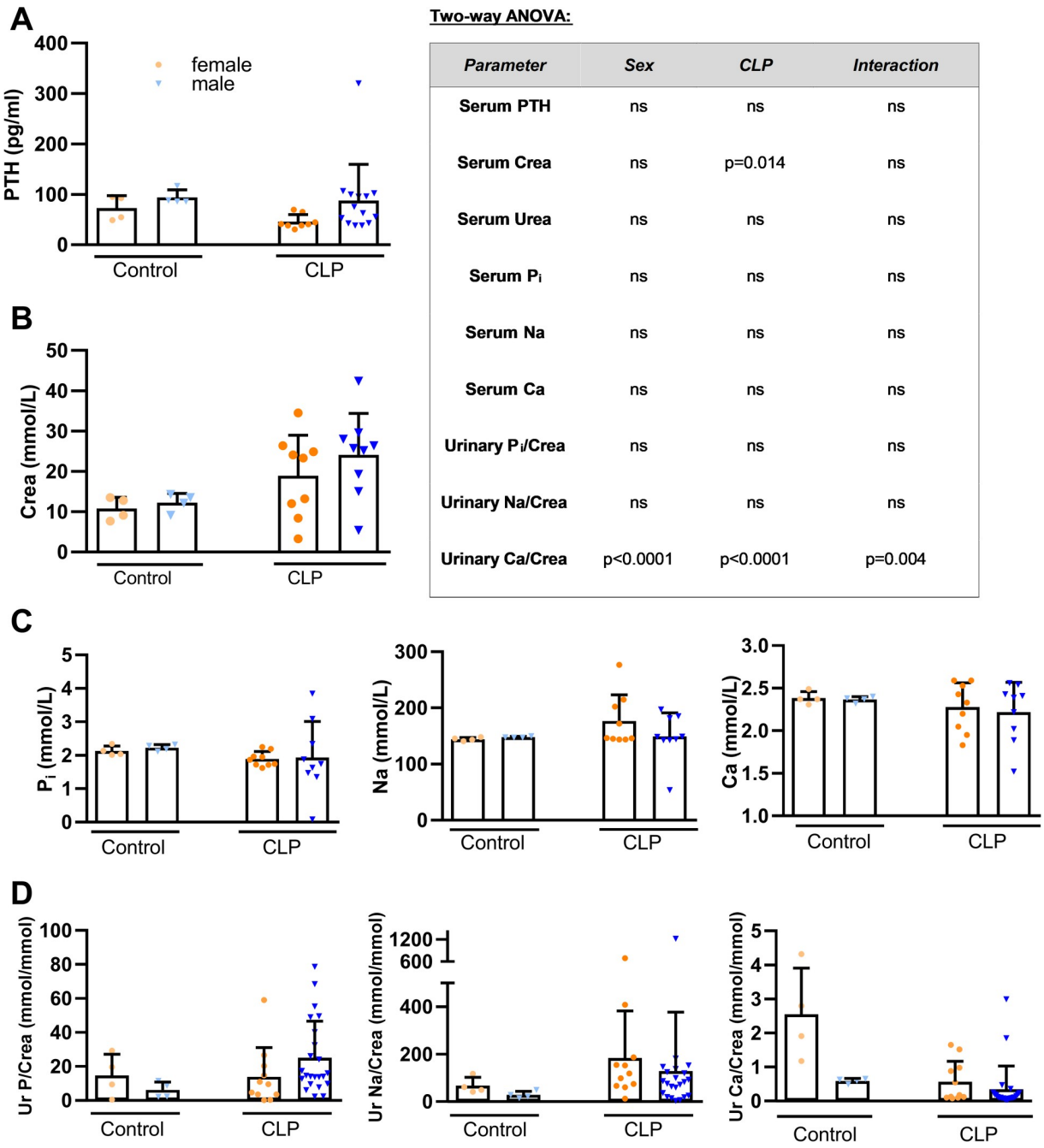

Two-way ANOVA:

Parameter	*Sex*	*CLP*	*Interaction*
Serum PTH	ns	ns	ns
Serum Crea	ns	p=0.014	ns
Serum Urea	ns	ns	ns
Serum P_i	ns	ns	ns
Serum Na	ns	ns	ns
Serum Ca	ns	ns	ns
Urinary P_i/Crea	ns	ns	ns
Urinary Na/Crea	ns	ns	ns
Urinary Ca/Crea	p<0.0001	p<0.0001	p=0.004

Fig 4. Circulating PTH concentration, serum creatinine, and mineral homeostasis in septic CLP mice. (A) Serum PTH level (healthy control female and male: n = 4 each; CLP female: n = 8, CLP male: n = 14), (B) serum creatinine (Crea), (C) serum phosphorus (P_i), sodium (Na) and calcium (Ca) levels (n = 4–9), (D) urinary phosphorus/creatinine (Ur P/Crea), sodium/creatinine (Ur Na/Crea) and calcium/creatinine (Ur Ca/Crea) (healthy control female and male: n = 4 each, CLP female: n = 11, CLP male: n = 22–23) in control and CLP mice, 48 h post-surgery. Bars are mean ± SD. Each symbol represents an individual sample. Inset shows results from two-way ANOVA. *, P<0.05 vs. healthy controls within same sex, Student's t-test with Welch correction.

https://doi.org/10.1371/journal.pone.0251317.g004

Discussion

The present study demonstrated for the first time that CLP-induced sepsis causes a profound increase in circulating intact FGF23 in mice. A number of studies reported that inflammatory

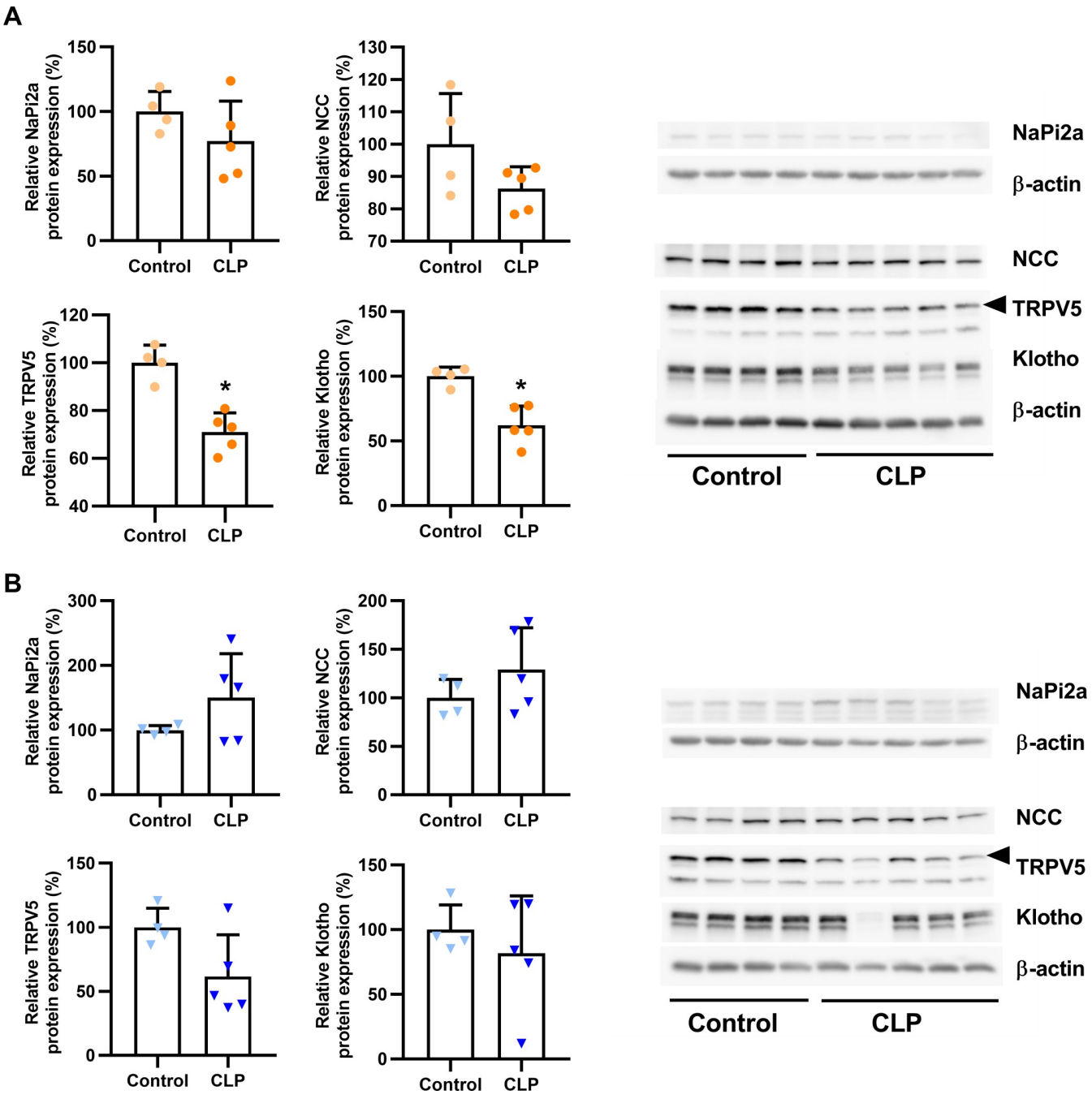

Fig 5. Effects of CLP-induced sepsis on the renal expression of phosphate-, sodium- and calcium-transporting proteins and of Klotho. Quantification and original western blot images of Napi2a, NCC, TRPV5 and Klotho protein expression detected in renal total membrane fractions of (A) female and (B) male healthy control and CLP mice, 48 h post-surgery. Each bar represents the mean ± SD of 4–5 mice per experimental group. Each symbol represents the mean of an individual sample measured on two membranes. *, $P<0.05$ vs. healthy control, Student's t-test with Welch correction.

https://doi.org/10.1371/journal.pone.0251317.g005

stimuli induce a rise in serum FGF23 [40,41,59,66,67]. However, these studies injected either cytokines, inactivated bacteria, or LPS into mice to cause an inflammatory response. The use of LPS to investigate altered physiology during endotoxemia has been a common practice. However, LPS is a classical TLR-4 agonist and induces a rapid and transient immune response

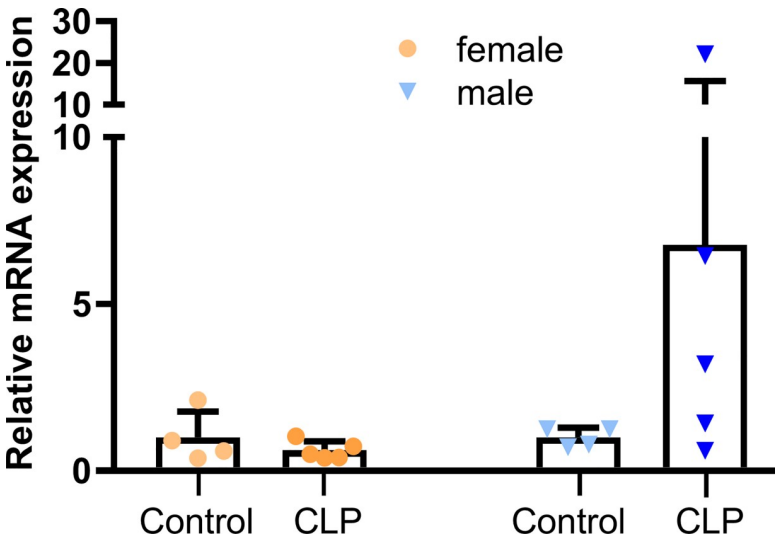

Fig 6. CLP-induced sepsis does not alter renal *1α-hydroxylase* mRNA expression. Relative renal mRNA expression of *1α-hydroxylase* measured by qRT-PCR in CLP mice (n = 5 female and male mice each) and healthy controls (n = 4 female and male mice each), 48 h post-surgery. Each bar represents the mean ± SD of 4–5 mice per experimental group. Each data point represents an individual animal.

https://doi.org/10.1371/journal.pone.0251317.g006

[48,68,69], which neither reflects the much milder and protracted elevation of circulating cytokines nor the hemodynamic changes occurring in human sepsis [46,70–75]. Therefore, CLP has been considered as a more appropriate recapitulation [46,47] of human abdominal sepsis including its general pathophysiology and the progressive release of cytokines in particular [48,49,69,71,76–78].

We observed that CLP-induced sepsis provoked a ~20-fold increase in circulating iFGF23 in both male and female mice, 48 h post-CLP. In agreement with the transient nature of LPS-induced endotoxemia, an FGF23 up-regulation of such magnitude and duration has never been reported in LPS-induced endotoxemia [36,41,59]. Our initial time-course experiment showed that the upregulation of circulating iFGF23 is preceded by a rapid increase in cleaved FGF23 within 6 h after CLP. The ratio of circulating intact to C-terminal FGF23, the latter encompassing both intact and cleaved FGF23, dropped precipitously within 6 h post-CLP, and remained suppressed until the 48 h time point. The latter finding suggests that CLP is associated with an increased cleavage of FGF23 and underscores the importance of measuring intact FGF23 at the protein level. The mechanisms stimulating cleavage of FGF23 in CLP mice are currently unknown and require further study.

In LPS injection models, the spleen has been identified as predominant site of FGF23 expression [36,41]. In contrast, David *et al*. postulated the bone as the main source for FGF23 synthesis during acute and chronic inflammation induced by heat-killed *Brucella abortus* or by IL-1β injection [40]. We found an upregulation of FGF23 protein only in the bone, but not in the spleen or liver of male and female CLP mice, 48 h post-CLP. In addition, *Fgf23* mRNA expression remained undetectable in the kidneys of male and female control and CLP mice. Thus, our data support the notion that the bone is the major site of FGF23 expression in CLP-induced polymicrobial sepsis.

Several clinical and experimental studies have shown a strong impact of sex and sex steroids on immune functions during physiological and pathophysiological conditions including sepsis [79–84]. Male sex and age [85] are the key risk factors for the development of sepsis [86–89]. In addition, males exhibit a higher morbidity and mortality from sepsis compared to females

[90–94]. However, in our experiments, we did not observe major sex effects on cytokine or circulating iFGF23 levels in CLP mice.

FGF23 is known to be a major regulator of mineral homeostasis. FGF23 downregulates apical membrane expression of the phosphate transporters Napi2a and NaPi2c in proximal renal tubules [17–21], and upregulates the sodium- and calcium transporting molecules NCC [24] and TRPV5 in distal tubules [23]. However, despite the very high serum FGF23 level in CLP mice, renal NaPi2a expression remained unchanged in both sexes. In contrast, Ikeda *et al.* [59] as well as Meurer & Höcherl [67] found a downregulation of renal NaPi2a protein expression in LPS-treated mice, together with increased PTH secretion. David *et al.* [40] observed an increase of serum PTH levels in acute inflammation experiments. However, chronic inflammation led to a reduced PTH secretion. A cytokine-dependent regulation of PTH secretion during inflammation has been reported in several studies [95,96]. Therefore, it is possible that a rapid, pronounced cytokine release such as seen after LPS injection triggers a different PTH secretion pattern compared with CLP. In the current study, we did not observe changes in serum PTH levels, 48 h after CLP. It is conceivable that the decreased renal expression of NaPi2a in LPS-treated mice observed in the aforementioned studies are mainly due to increased PTH secretion rather than the elevated iFGF23.

In agreement with the unchanged serum concentration of sodium, CLP mice of both sexes did not show altered renal NCC protein expression compared to control mice in our study. Similarly, Olesen *et al.* [97] found unchanged expression of NCC in LPS-treated rats. However, the latter authors observed reduced serum sodium levels and increased urinary sodium excretion, which was accompanied by a downregulation of other sodium transporters across different renal compartments.

In our study, CLP mice, regardless of sex, exhibited an unchanged total serum calcium concentration, relative to healthy controls. In addition, CLP females but not males showed a reduced urinary calcium excretion, compared to healthy control mice. The renal expression of TRPV5 failed to provide an explanation for these findings, given that we observed a downregulation of TRPV5 abundance in septic females, but unchanged expression in septic males. Therefore, it is likely that other factors over-compensated for the reduced TRPV5 expression in female mice. A possible candidate might be TRPV6, which we did not measure. Meurer & Höcherl [67] have shown that LPS directly upregulates TRPV5 and 6 expression in primary renal epithelial cells. Therefore, it is possible that CLP differentially regulates TRPV5 and 6 in female mice. In addition, it is well known that the open probability of TRPV5 is regulated by endocrine and paracrine factors [98–100], so that the protein abundance not necessarily reflects the functional activity.

An important question in this context is why the increased circulating FGF23 did not downregulate NaPi2a, and failed to upregulate NCC and TRPV5 expression in the kidney of septic mice. In other words, why was sepsis associated with an apparent renal FGF23 resistance? It has been recently shown that LPS injection resulted in a ~90% reduction in renal function as measured by creatinine clearance in mice [67]. Hence, sepsis-induced acute kidney injury might render the kidney FGF23 resistant. In the current study, we could not assess creatinine clearance, because we collected only spontaneous urine. However, CLP was associated with increased serum creatinine, reflecting the CLP-induced decline in kidney function. FGF23 signaling requires the presence of the co-receptor Klotho [25,30–32] and there is convincing evidence that renal Klotho protein expression is reduced in septic patients with AKI [101], in septic foals [102], and in experimental sepsis models [101,103–106]. Similarly, we found diminished renal Klotho expression in female CLP mice. However, male CLP mice did not generally exhibit a significant decrease in Klotho protein abundance. Other studies using male mice showed a reduction of Klotho expression after inflammatory stimuli [101,106–108].

Therefore, we do not have a good explanation for the sex difference in Klotho expression in CLP mice. Nevertheless, reduced Klotho protein expression is one of the most likely scenarios for the renal FGF23 resistance observed in septic patients and experimental sepsis models.

In conclusion, our data demonstrate a robust increase in circulating iFGF23 in mice of both sexes in the acute phase of polymicrobial sepsis. The bone appears to be the major source of FGF23 in acute CLP sepsis. Because mineral homeostasis did not show major alterations in CLP mice, the biological function of the high circulating iFGF23 in acute sepsis remains unclear. Several lines of evidence support the role of FGF23 as an immune-regulatory molecule. It has been shown that FGF23 is able to regulate cytokine production in macrophages [9,36] and hepatocytes [37]. Furthermore, a transcriptome analysis in CKD mice revealed several FGF23-responsive pro-inflammatory pathways in the kidney, including TGF-β, TNF-α, and IL-1β signaling pathways [109]. Therefore, based on current knowledge [110,111], iFGF23 may serve as a positive feedback signal between various inflammatory processes and the bone. This warrants further studies aimed at delineating the pathophysiological role of FGF23 in sepsis.

Supporting information

S1 Raw images.
(PDF)

Acknowledgments

We thank Alexandra Petric and Claudia Bergow for excellent technical assistance, and Alexander Tichy for advice regarding the statistical analyses. We also gratefully appreciate the assistance of T. Spenlingwimmer in animal experiments. Additionally, the authors thank the University Clinic for Swine on the campus of the University of Veterinary Medicine Vienna for providing us with the Bio-Plex 200 System and in particular Lisa Reiter for her excellent introduction to the Luminex analysis. Olena Andrukhova passed away before the submission of this manuscript. RGE accepts responsibility for the integrity and validity of the data collected and analyzed.

Author Contributions

Conceptualization: Marcin F. Osuchowski, Reinhold G. Erben, Olena Andrukhova.

Data curation: Jessica Bayer, Ravikumar Vaghela, Susanne Drechsler, Marcin F. Osuchowski.

Formal analysis: Jessica Bayer.

Funding acquisition: Reinhold G. Erben, Olena Andrukhova.

Project administration: Reinhold G. Erben, Olena Andrukhova.

Supervision: Marcin F. Osuchowski, Reinhold G. Erben, Olena Andrukhova.

Validation: Susanne Drechsler, Marcin F. Osuchowski, Reinhold G. Erben.

Visualization: Jessica Bayer.

Writing – original draft: Jessica Bayer.

Writing – review & editing: Jessica Bayer, Ravikumar Vaghela, Susanne Drechsler, Marcin F. Osuchowski, Reinhold G. Erben.

References

1. Liu S, Tang W, Zhou J, Vierthaler L, Quarles LD. Distinct roles for intrinsic osteocyte abnormalities and systemic factors in regulation of FGF23 and bone mineralization in Hyp mice. Am J Physiol Endocrinol Metab. 2007; 293(6):E1636–44. https://doi.org/10.1152/ajpendo.00396.2007 PMID: 17848631.
2. Yoshiko Y, Wang H, Minamizaki T, Ijuin C, Yamamoto R, Suemune S, et al. Mineralized tissue cells are a principal source of FGF23. Bone. 2007; 40(6):1565–73. https://doi.org/10.1016/j.bone.2007.01.017 PMID: 17350357.
3. Martin A, David V, Quarles LD. Regulation and function of the FGF23/klotho endocrine pathways. Physiol Rev. 2012; 92(1):131–55. https://doi.org/10.1152/physrev.00002.2011 PMID: 22298654.
4. Han X, Yang J, Li L, Huang J, King G, Quarles LD. Conditional Deletion of Fgfr1 in the Proximal and Distal Tubule Identifies Distinct Roles in Phosphate and Calcium Transport. PLoS ONE. 2016; 11(2): e0147845. https://doi.org/10.1371/journal.pone.0147845 PMID: 26839958.
5. Perwad F, Azam N, Zhang MYH, Yamashita T, Tenenhouse HS, Portale AA. Dietary and serum phosphorus regulate fibroblast growth factor 23 expression and 1,25-dihydroxyvitamin D metabolism in mice. Endocrinology. 2005; 146(12):5358–64. https://doi.org/10.1210/en.2005-0777 PMID: 16123154.
6. Saito H, Maeda A, Ohtomo S-I, Hirata M, Kusano K, Kato S, et al. Circulating FGF-23 is regulated by 1alpha,25-dihydroxyvitamin D3 and phosphorus in vivo. J Biol Chem. 2005; 280(4):2543–9. https://doi.org/10.1074/jbc.M408903200 PMID: 15531762.
7. Burnett S-AM, Gunawardene SC, Bringhurst FR, Jüppner H, Lee H, Finkelstein JS. Regulation of C-terminal and intact FGF-23 by dietary phosphate in men and women. J Bone Miner Res. 2006; 21 (8):1187–96. https://doi.org/10.1359/jbmr.060507 PMID: 16869716.
8. Quinn SJ, Thomsen ARB, Pang JL, Kantham L, Bräuner-Osborne H, Pollak M, et al. Interactions between calcium and phosphorus in the regulation of the production of fibroblast growth factor 23 in vivo. Am J Physiol Endocrinol Metab. 2013; 304(3):E310–20. https://doi.org/10.1152/ajpendo.00460.2012 PMID: 23233539.
9. Han X, Li L, Yang J, King G, Xiao Z, Quarles LD. Counter-regulatory paracrine actions of FGF-23 and 1,25(OH)2 D in macrophages. FEBS Lett. 2016; 590(1):53–67. https://doi.org/10.1002/1873-3468.12040 PMID: 26762170.
10. Liu S, Tang W, Zhou J, Stubbs JR, Luo Q, Pi M, et al. Fibroblast growth factor 23 is a counter-regulatory phosphaturic hormone for vitamin D. J Am Soc Nephrol. 2006; 17(5):1305–15. https://doi.org/10.1681/ASN.2005111185 PMID: 16597685.
11. Kaneko I, Saini RK, Griffin KP, Whitfield GK, Haussler MR, Jurutka PW. FGF23 gene regulation by 1,25-dihydroxyvitamin D: opposing effects in adipocytes and osteocytes. J Endocrinol. 2015; 226 (3):155–66. https://doi.org/10.1530/JOE-15-0225 PMID: 26148725.
12. Lavi-Moshayoff V, Wasserman G, Meir T, Silver J, Naveh-Many T. PTH increases FGF23 gene expression and mediates the high-FGF23 levels of experimental kidney failure: a bone parathyroid feedback loop. Am J Physiol Renal Physiol. 2010; 299(4):F882–9. https://doi.org/10.1152/ajprenal.00360.2010 PMID: 20685823.
13. Rhee Y, Bivi N, Farrow E, Lezcano V, Plotkin LI, White KE, et al. Parathyroid hormone receptor signaling in osteocytes increases the expression of fibroblast growth factor-23 in vitro and in vivo. Bone. 2011; 49(4):636–43. https://doi.org/10.1016/j.bone.2011.06.025 PMID: 21726676.
14. Meir T, Durlacher K, Pan Z, Amir G, Richards WG, Silver J, et al. Parathyroid hormone activates the orphan nuclear receptor Nurr1 to induce FGF23 transcription. Kidney Int. 2014; 86(6):1106–15. https://doi.org/10.1038/ki.2014.215 PMID: 24940803.
15. Fan Y, Bi R, Densmore MJ, Sato T, Kobayashi T, Yuan Q, et al. Parathyroid hormone 1 receptor is essential to induce FGF23 production and maintain systemic mineral ion homeostasis. FASEB J. 2015; 30(1):428–40. https://doi.org/10.1096/fj.15-278184 PMID: 26428657.
16. Knab VM, Corbin B, Andrukhova O, Hum JM, Ni P, Rabadi S, et al. Acute Parathyroid Hormone Injection Increases C-Terminal but Not Intact Fibroblast Growth Factor 23 Levels. Endocrinology. 2017; 158(5):1130–9. https://doi.org/10.1210/en.2016-1451 PMID: 28324013.
17. Shimada T, Hasegawa H, Yamazaki Y, Muto T, Hino R, Takeuchi Y, et al. FGF-23 is a potent regulator of vitamin D metabolism and phosphate homeostasis. J Bone Miner Res. 2004; 19(3):429–35. https://doi.org/10.1359/JBMR.0301264 PMID: 15040831.
18. Shimada T, Urakawa I, Yamazaki Y, Hasegawa H, Hino R, Yoneya T, et al. FGF-23 transgenic mice demonstrate hypophosphatemic rickets with reduced expression of sodium phosphate cotransporter type IIa. Biochem Biophys Res Commun. 2004; 314(2):409–14. https://doi.org/10.1016/j.bbrc.2003.12.102 PMID: 14733920

19. Baum M, Schiavi S, Dwarakanath V, Quigley R. Effect of fibroblast growth factor-23 on phosphate transport in proximal tubules. Kidney Int. 2005; 68(3):1148–53. https://doi.org/10.1111/j.1523-1755.2005.00506.x PMID: 16105045.

20. Shimada T, Yamazaki Y, Takahashi M, Hasegawa H, Urakawa I, Oshima T, et al. Vitamin D receptor-independent FGF23 actions in regulating phosphate and vitamin D metabolism. Am J Physiol Renal Physiol. 2005; 289(5):F1088–95. https://doi.org/10.1152/ajprenal.00474.2004 PMID: 15998839.

21. Andrukhova O, Zeitz U, Goetz R, Mohammadi M, Lanske B, Erben RG. FGF23 acts directly on renal proximal tubules to induce phosphaturia through activation of the ERK1/2-SGK1 signaling pathway. Bone. 2012; 51(3):621–8. https://doi.org/10.1016/j.bone.2012.05.015 PMID: 22647968.

22. Wikvall K. Cytochrome P450 enzymes in the bioactivation of vitamin D to its hormonal form (Review). Int J Mol Med. 2001. https://doi.org/10.3892/ijmm.7.2.201 PMID: 11172626

23. Andrukhova O, Smorodchenko A, Egerbacher M, Streicher C, Zeitz U, Goetz R, et al. FGF23 promotes renal calcium reabsorption through the TRPV5 channel. EMBO J. 2014; 33(3):229–46. https://doi.org/10.1002/embj.201284188 PMID: 24434184.

24. Andrukhova O, Slavic S, Smorodchenko A, Zeitz U, Shalhoub V, Lanske B, et al. FGF23 regulates renal sodium handling and blood pressure. EMBO Mol Med. 2014; 6(6):744–59. https://doi.org/10.1002/emmm.201303716 PMID: 24797667.

25. Urakawa I, Yamazaki Y, Shimada T, Iijima K, Hasegawa H, Okawa K, et al. Klotho converts canonical FGF receptor into a specific receptor for FGF23. Nature. 2006; 444(7120):770–4. https://doi.org/10.1038/nature05315 PMID: 17086194.

26. Gattineni J, Twombley K, Goetz R, Mohammadi M, Baum M. Regulation of serum 1,25(OH)2Vitamin D3 levels by fibroblast growth factor 23 is mediated by FGF receptors 3 and 4. Am J Physiol Renal Physiol. 2011; 301(2):F371–7. https://doi.org/10.1152/ajprenal.00740.2010 PMID: 21561999.

27. Li H, Martin A, David V, Quarles LD. Compound deletion of Fgfr3 and Fgfr4 partially rescues the Hyp mouse phenotype. Am J Physiol Endocrinol Metab. 2011; 300(3):E508–17. https://doi.org/10.1152/ajpendo.00499.2010 PMID: 21139072.

28. Gattineni J, Alphonse P, Zhang Q, Mathews N, Bates CM, Baum M. Regulation of renal phosphate transport by FGF23 is mediated by FGFR1 and FGFR4. Am J Physiol Renal Physiol. 2014; 306(3):F351–8. https://doi.org/10.1152/ajprenal.00232.2013 PMID: 24259513.

29. Kuro-o M, Matsumura Y, Aizawa H, Kawaguchi H, Suga T, Utsugi T, et al. Mutation of the mouse klotho gene leads to a syndrome resembling ageing. Nature. 1997; 390(6655):45–51. https://doi.org/10.1038/36285 PMID: 9363890.

30. Kurosu H, Ogawa Y, Miyoshi M, Yamamoto M, Nandi A, Rosenblatt KP, et al. Regulation of fibroblast growth factor-23 signaling by klotho. J Biol Chem. 2006; 281(10):6120–3. https://doi.org/10.1074/jbc.C500457200 PMID: 16436388.

31. Goetz R, Ohnishi M, Kir S, Kurosu H, Wang L, Pastor J, et al. Conversion of a paracrine fibroblast growth factor into an endocrine fibroblast growth factor. J Biol Chem. 2012; 287(34):29134–46. https://doi.org/10.1074/jbc.M112.342980 PMID: 22733815.

32. Chen G, Liu Y, Goetz R, Fu L, Jayaraman S, Hu M-C, et al. α-Klotho is a non-enzymatic molecular scaffold for FGF23 hormone signalling. Nature. 2018; 553(7689):461–6. https://doi.org/10.1038/nature25451 PMID: 29342138.

33. Imura A, Iwano A, Tohyama O, Tsuji Y, Nozaki K, Hashimoto N, et al. Secreted Klotho protein in sera and CSF: implication for post-translational cleavage in release of Klotho protein from cell membrane. FEBS Lett. 2004; 565(1–3):143–7. https://doi.org/10.1016/j.febslet.2004.03.090 PMID: 15135068.

34. Bloch L, Sineshchekova O, Reichenbach D, Reiss K, Saftig P, Kuro-o M, et al. Klotho is a substrate for alpha-, beta- and gamma-secretase. FEBS Lett. 2009; 583(19):3221–4. https://doi.org/10.1016/j.febslet.2009.09.009 PMID: 19737556.

35. Chen C-D, Podvin S, Gillespie E, Leeman SE, Abraham CR. Insulin stimulates the cleavage and release of the extracellular domain of Klotho by ADAM10 and ADAM17. Proc Natl Acad Sci U S A. 2007; 104(50):19796–801. https://doi.org/10.1073/pnas.0709805104 PMID: 18056631.

36. Masuda Y, Ohta H, Morita Y, Nakayama Y, Miyake A, Itoh N, et al. Expression of Fgf23 in activated dendritic cells and macrophages in response to immunological stimuli in mice. Biol Pharm Bull. 2015; 38(5):687–93. https://doi.org/10.1248/bpb.b14-00276 PMID: 25739891.

37. Singh S, Grabner A, Yanucil C, Schramm K, Czaya B, Krick S, et al. Fibroblast growth factor 23 directly targets hepatocytes to promote inflammation in chronic kidney disease. Kidney Int. 2016; 90(5):985–96. https://doi.org/10.1016/j.kint.2016.05.019 PMID: 27457912.

38. Ito N, Wijenayaka AR, Prideaux M, Kogawa M, Ormsby RT, Evdokiou A, et al. Regulation of FGF23 expression in IDG-SW3 osteocytes and human bone by pro-inflammatory stimuli. Mol Cell Endocrinol. 2015; 399:208–18. https://doi.org/10.1016/j.mce.2014.10.007 PMID: 25458698.

39. Yamazaki M, Kawai M, Miyagawa K, Ohata Y, Tachikawa K, Kinoshita S, et al. Interleukin-1-induced acute bone resorption facilitates the secretion of fibroblast growth factor 23 into the circulation. J Bone Miner Metab. 2015; 33(3):342–54. https://doi.org/10.1007/s00774-014-0598-2 PMID: 24996526.

40. David V, Martin A, Isakova T, Spaulding C, Qi L, Ramirez V, et al. Inflammation and functional iron deficiency regulate fibroblast growth factor 23 production. Kidney Int. 2016; 89(1):135–46. https://doi.org/10.1038/ki.2015.290 PMID: 26535997.

41. Bansal S, Friedrichs WE, Velagapudi C, Feliers D, Khazim K, Horn D, et al. Spleen contributes significantly to increased circulating levels of fibroblast growth factor 23 in response to lipopolysaccharide-induced inflammation. Nephrol Dial Transplant. 2017; 32(6):960–8. https://doi.org/10.1093/ndt/gfw376 PMID: 27836924.

42. Leaf DE, Waikar SS, Wolf M, Cremers S, Bhan I, Stern L. Dysregulated mineral metabolism in patients with acute kidney injury and risk of adverse outcomes. Clin Endocrinol (Oxf). 2013; 79(4):491–8. https://doi.org/10.1111/cen.12172 PMID: 23414198.

43. Singer M, Deutschman CS, Seymour CW, Shankar-Hari M, Annane D, Bauer M, et al. The Third International Consensus Definitions for Sepsis and Septic Shock (Sepsis-3). JAMA [Internet]. 2016; 315 (8):801–10. Available from: https://jamanetwork.com/journals/jama/articlepdf/2492881/jsc160002.pdf. https://doi.org/10.1001/jama.2016.0287 PMID: 26903338

44. Rudd KE, Johnson SC, Agesa KM, Shackelford KA, Tsoi D, Kievlan DR, et al. Global, regional, and national sepsis incidence and mortality, 1990–2017: analysis for the Global Burden of Disease Study. Lancet. 2020; 395(10219):200–11. https://doi.org/10.1016/S0140-6736(19)32989-7 PMID: 31954465.

45. Vincent J-L, Marshall JC, Ñamendys-Silva SA, François B, Martin-Loeches I, Lipman J, et al. Assessment of the worldwide burden of critical illness: the Intensive Care Over Nations (ICON) audit. The Lancet Respiratory Medicine. 2014; 2(5):380–6. https://doi.org/10.1016/S2213-2600(14)70061-X PMID: 24740011

46. Wichterman KA, Baue AE, Chaudry IH. Sepsis and septic shock—A review of laboratory models and a proposal. Journal of Surgical Research. 1980; 29(2):189–201. https://doi.org/10.1016/0022-4804(80)90037-2 PMID: 6997619

47. Parker SJ, Watkins PE. Experimental models of gram-negative sepsis. Br J Surg. 2001; 88(1):22–30. https://doi.org/10.1046/j.1365-2168.2001.01632.x PMID: 11136305.

48. Buras JA, Holzmann B, Sitkovsky M. Animal models of sepsis: setting the stage. Nat Rev Drug Discov. 2005; 4(10):854–65. https://doi.org/10.1038/nrd1854 PMID: 16224456.

49. Doi K, Leelahavanichkul A, Yuen PST, Star RA. Animal models of sepsis and sepsis-induced kidney injury. J Clin Invest. 2009; 119(10):2868–78. https://doi.org/10.1172/JCI39421 PMID: 19805915.

50. Rademann P, Weidinger A, Drechsler S, Meszaros A, Zipperle J, Jafarmadar M, et al. Mitochondria-Targeted Antioxidants SkQ1 and MitoTEMPO Failed to Exert a Long-Term Beneficial Effect in Murine Polymicrobial Sepsis. Oxid Med Cell Longev. 2017; 2017:6412682. https://doi.org/10.1155/2017/6412682 PMID: 29104729.

51. Drechsler S, Weixelbaumer K, Raeven P, Jafarmadar M, Khadem A, van Griensven M, et al. Relationship between age/gender-induced survival changes and the magnitude of inflammatory activation and organ dysfunction in post-traumatic sepsis. PLoS ONE. 2012; 7(12):e51457. https://doi.org/10.1371/journal.pone.0051457 PMID: 23251540.

52. Weixelbaumer KM, Raeven P, Redl H, van Griensven M, Bahrami S, Osuchowski MF. Repetitive low-volume blood sampling method as a feasible monitoring tool in a mouse model of sepsis. Shock. 2010; 34(4):420–6. https://doi.org/10.1097/SHK.0b013e3181dc0918 PMID: 20610942.

53. Jiang X, Ye M, Jiang X, Liu G, Feng S, Cui L, et al. Method development of efficient protein extraction in bone tissue for proteome analysis. J Proteome Res. 2007; 6(6):2287–94. https://doi.org/10.1021/pr070056t PMID: 17488005.

54. Bienaimé F, Ambolet A, Aussilhou B, Brazier F, Fouchard M, Viau A, et al. Hepatic Production of Fibroblast Growth Factor 23 in Autosomal Dominant Polycystic Kidney Disease. J Clin Endocrinol Metab. 2018; 103(6):2319–28. https://doi.org/10.1210/jc.2018-00123 PMID: 29618028.

55. Zanchi C, Locatelli M, Benigni A, Corna D, Tomasoni S, Rottoli D, et al. Renal expression of FGF23 in progressive renal disease of diabetes and the effect of ACE inhibitor. PLoS ONE. 2013; 8(8):e70775. https://doi.org/10.1371/journal.pone.0070775 PMID: 23967103.

56. Shimada T, Mizutani S, Muto T, Yoneya T, Hino R, Takeda S, et al. Cloning and characterization of FGF23 as a causative factor of tumor-induced osteomalacia. Proceedings of the National Academy of Sciences. 2001; 98(11):6500–5. https://doi.org/10.1073/pnas.101545198 PMID: 11344269.

57. Spichtig D, Zhang H, Mohebbi N, Pavik I, Petzold K, Stange G, et al. Renal expression of FGF23 and peripheral resistance to elevated FGF23 in rodent models of polycystic kidney disease. Kidney Int. 2014; 85(6):1340–50. https://doi.org/10.1038/ki.2013.526 PMID: 24402093.

58. Sugiura H, Matsushita A, Futaya M, Teraoka A, Akiyama K-I, Usui N, et al. Fibroblast growth factor 23 is upregulated in the kidney in a chronic kidney disease rat model. PLoS ONE. 2018; 13(3):e0191706. https://doi.org/10.1371/journal.pone.0191706 PMID: 29518087.

59. Ikeda S, Yamamoto H, Masuda M, Takei Y, Nakahashi O, Kozai M, et al. Downregulation of renal type IIa sodium-dependent phosphate cotransporter during lipopolysaccharide-induced acute inflammation. Am J Physiol Renal Physiol. 2014; 306(7):F744–50. https://doi.org/10.1152/ajprenal.00474.2013 PMID: 24500689.

60. Gustot T. Multiple organ failure in sepsis: prognosis and role of systemic inflammatory response. Curr Opin Crit Care. 2011; 17(2):153–9. https://doi.org/10.1097/MCC.0b013e328344b446 PMID: 21346564.

61. Doi K. Role of kidney injury in sepsis. J Intensive Care. 2016; 4:17. https://doi.org/10.1186/s40560-016-0146-3 PMID: 27011788.

62. Poston JT, Koyner JL. Sepsis associated acute kidney injury. BMJ. 2019; 364:k4891. https://doi.org/10.1136/bmj.k4891 PMID: 30626586.

63. Höcherl K, Schmidt C, Kurt B, Bucher M. Inhibition of NF-kappaB ameliorates sepsis-induced downregulation of aquaporin-2/V2 receptor expression and acute renal failure in vivo. Am J Physiol Renal Physiol. 2010; 298(1):F196–204. https://doi.org/10.1152/ajprenal.90607.2008 PMID: 19828675.

64. Rodrigues CE, Sanches TR, Volpini RA, Shimizu MHM, Kuriki PS, Camara NOS, et al. Effects of continuous erythropoietin receptor activator in sepsis-induced acute kidney injury and multi-organ dysfunction. PLoS ONE. 2012; 7(1):e29893. https://doi.org/10.1371/journal.pone.0029893 PMID: 22235348.

65. Zhao W-Y, Zhang L, Sui M-X, Zhu Y-H, Zeng L. Protective effects of sirtuin 3 in a murine model of sepsis-induced acute kidney injury. Sci Rep. 2016; 6:33201. https://doi.org/10.1038/srep33201 PMID: 27620507.

66. Onal M, Carlson AH, Thostenson JD, Benkusky NA, Meyer MB, Lee SM, et al. A Novel Distal Enhancer Mediates Inflammation-, PTH-, and Early Onset Murine Kidney Disease-Induced Expression of the Mouse Fgf23 Gene. JBMR Plus. 2018; 2(1):32–47. https://doi.org/10.1002/jbm4.10023 PMID: 29527594.

67. Meurer M, Höcherl K. Endotoxaemia differentially regulates the expression of renal Ca2+ transport proteins in mice. Acta Physiol (Oxf). 2019; 225(1):e13175. https://doi.org/10.1111/apha.13175 PMID: 30133162.

68. Remick DG, Newcomb DE, Bolgos GL, Call DR. COMPARISON OF THE MORTALITY AND INFLAMMATORY RESPONSE OF TWO MODELS OF SEPSIS: LIPOPOLYSACCHARIDE VS. CECAL LIGATION AND PUNCTURE. Shock. 2000; 13(2):110–6. https://doi.org/10.1097/00024382-200013020-00004 PMID: 10670840

69. Seemann S, Zohles F, Lupp A. Comprehensive comparison of three different animal models for systemic inflammation. J Biomed Sci. 2017; 24(1):60. https://doi.org/10.1186/s12929-017-0370-8 PMID: 28836970.

70. Fink MP, Heard SO. Laboratory models of sepsis and septic shock. Journal of Surgical Research. 1990; 49(2):186–96. https://doi.org/10.1016/0022-4804(90)90260-9 PMID: 2199735

71. Deitch EA. ANIMAL MODELS OF SEPSIS AND SHOCK. Shock. 1998; 9(1):1–11. https://doi.org/10.1097/00024382-199801000-00001 PMID: 9466467

72. Remick DG, Ward PA. EVALUATION OF ENDOTOXIN MODELS FOR THE STUDY OF SEPSIS. Shock. 2005; 24(Supplement 1):7–11. https://doi.org/10.1097/01.shk.0000191384.34066.85 PMID: 16374366

73. Nemzek JA, Hugunin KMS, Opp MR. Modeling Sepsis in the Laboratory: Merging Sound Science with Animal Well-Being. Comp Med. 20; 58(2):120–8. PMID: 18524169.

74. Dejager L, Pinheiro I, Dejonckheere E, Libert C. Cecal ligation and puncture: the gold standard model for polymicrobial sepsis? Trends Microbiol. 2011; 19(4):198–208. https://doi.org/10.1016/j.tim.2011.01.001 PMID: 21296575.

75. Lewis AJ, Seymour CW, Rosengart MR. Current Murine Models of Sepsis. Surg Infect (Larchmt). 2016; 17(4):385–93. https://doi.org/10.1089/sur.2016.021 PMID: 27305321.

76. Ebong S, Call D, Nemzek J, Bolgos G, Newcomb D, Remick D. Immunopathologic Alterations in Murine Models of Sepsis of Increasing Severity. Infect Immun. 1999; 67(12):6603–10. PMID: 10569781.

77. Yang S, Chung C-S, Ayala A, Chaudry IH, Wang P. Differential alterations in cardiovascular responses during the progression of polymicrobial sepsis in the mouse. Shock. 2002; 17(1):55–60. https://doi.org/10.1097/00024382-200201000-00010 PMID: 11795670.

78. Tao W, Deyo DJ, Traber DL, Johnston WE, Sherwood ER. Hemodynamic and cardiac contractile function during sepsis caused by cecal ligation and puncture in mice. Shock. 2004; 21(1):31–7. https://doi.org/10.1097/01.shk.0000101673.49265.5d PMID: 14676681.

79. Bösch F, Angele MK, Chaudry IH. Gender differences in trauma, shock and sepsis. Mil Med Res. 2018; 5(1):35. https://doi.org/10.1186/s40779-018-0182-5 PMID: 30360757.

80. Knöferl MW, Angele MK, Diodato M d., Schwacha MG, Ayala A, Cioffi WG, et al. Female Sex Hormones Regulate Macrophage Function After Trauma-Hemorrhage and Prevent Increased Death Rate From Subsequent Sepsis. Ann Surg. 2002; 235(1):105–12. https://doi.org/10.1097/00000658-200201000-00014 PMID: 11753049.

81. Angele MK, Frantz MC, Chaudry IH. Gender and sex hormones influence the response to trauma and sepsis: potential therapeutic approaches. Clinics. 2006; 61(5). https://doi.org/10.1590/s1807-59322006000500017 PMID: 17072448

82. Christaki E, Opal SM, Keith JC, Kessinian N, Palardy JE, Parejo NA, et al. Estrogen receptor beta agonism increases survival in experimentally induced sepsis and ameliorates the genomic sepsis signature: a pharmacogenomic study. J Infect Dis. 2010; 201(8):1250–7. https://doi.org/10.1086/651276 PMID: 20205571.

83. Sakiani S, Olsen NJ, Kovacs WJ. Gonadal steroids and humoral immunity. Nat Rev Endocrinol. 2013; 9(1):56–62. https://doi.org/10.1038/nrendo.2012.206 PMID: 23183675.

84. Angele MK, Pratschke S, Hubbard WJ, Chaudry IH. Gender differences in sepsis: cardiovascular and immunological aspects. Virulence. 2014; 5(1):12–9. https://doi.org/10.4161/viru.26982 PMID: 24193307.

85. Martin GS, Mannino DM, Moss M. The effect of age on the development and outcome of adult sepsis*. Crit Care Med. 2006; 34(1):15–21. https://doi.org/10.1097/01.ccm.0000194535.82812.ba PMID: 16374151

86. Oberholzer A, Keel M, Zellweger R, Steckholzer U, Trentz O, Ertel W. Incidence of septic complications and multiple organ failure in severely injured patients is sex specific. J Trauma. 2000; 48(5):932–7. https://doi.org/10.1097/00005373-200005000-00019 PMID: 10823539.

87. Maio A de, Torres MB, Reeves RH. Genetic determinants influencing the response to injury, inflammation, and sepsis. Shock. 2005; 23(1):11–7. https://doi.org/10.1097/01.shk.0000144134.03598.c5 PMID: 15614125.

88. Frink M, Pape H-C, van Griensven M, Krettek C, Chaudry IH, Hildebrand F. Influence of sex and age on mods and cytokines after multiple injuries. Shock. 2007; 27(2):151–6. https://doi.org/10.1097/01.shk.0000239767.64786.de PMID: 17224789.

89. Kisat M, Villegas CV, Onguti S, Zafar SN, Latif A, Efron DT, et al. Predictors of sepsis in moderately severely injured patients: an analysis of the National Trauma Data Bank. Surg Infect (Larchmt). 2013; 14(1):62–8. https://doi.org/10.1089/sur.2012.009 PMID: 23461696.

90. Zellweger R, Wichmann MW, Ayala A, Stein S, DeMaso CM, Chaudry IH. Females in proestrus state maintain splenic immune functions and tolerate sepsis better than males. Crit Care Med. 1997; 25(1):106–10. https://doi.org/10.1097/00003246-199701000-00021 PMID: 8989185.

91. Schröder J. Gender Differences in Human Sepsis. Arch Surg. 1998; 133(11):1200. https://doi.org/10.1001/archsurg.133.11.1200 PMID: 9820351

92. Diodato MD, Knöferl MW, Schwacha MG, Bland KI, Chaudry IH. Gender differences in the inflammatory response and survival following haemorrhage and subsequent sepsis. Cytokine. 2001; 14(3):162–9. https://doi.org/10.1006/cyto.2001.0861 PMID: 11396994.

93. Drechsler S, Weixelbaumer K, Raeven P, Jafarmadar M, Khadem A, van Griensven M, et al. Relationship between age/gender-induced survival changes and the magnitude of inflammatory activation and organ dysfunction in post-traumatic sepsis. PLoS ONE. 2012; 7(12):e51457. https://doi.org/10.1371/journal.pone.0051457 PMID: 23251540.

94. Chen J, Chiazza F, Collino M, Patel NSA, Coldewey SM, Thiemermann C. Gender dimorphism of the cardiac dysfunction in murine sepsis: signalling mechanisms and age-dependency. PLoS ONE. 2014; 9(6):e100631. https://doi.org/10.1371/journal.pone.0100631 PMID: 24945834.

95. af EE, Benson L, Hällgren R, Wide L, Ljunghall S. Impaired secretion of parathyroid hormone in patients with rheumatoid arthritis: relationship to inflammatory activity. Clin Endocrinol (Oxf) [Internet]. 1990; 32(3). Available from: https://pubmed.ncbi.nlm.nih.gov/2111747/.

96. Augustine MV, Leonard MB, Thayu M, Baldassano RN, Boer IH de, Shults J, et al. Changes in Vitamin D-Related Mineral Metabolism After Induction With Anti-Tumor Necrosis Factor-α Therapy in Crohn's Disease. J Clin Endocrinol Metab. 2014; 99(6):E991–8. https://doi.org/10.1210/jc.2013-3846 PMID: 24617709.

97. Olesen ETB, Seigneux S de, Wang G, Lütken SC, Frøkiaer J, Kwon T-H, et al. Rapid and segmental specific dysregulation of AQP2, S256-pAQP2 and renal sodium transporters in rats with LPS-induced endotoxaemia. Nephrol Dial Transplant. 2009; 24(8):2338–49. https://doi.org/10.1093/ndt/gfp011 PMID: 19193739.

98. Groot T de Bindels RJM, Hoenderop JGJ. TRPV5: an ingeniously controlled calcium channel. Kidney Int. 2008; 74(10):1241–6. https://doi.org/10.1038/ki.2008.320 PMID: 18596722.

99. Boros S, Bindels RJM, Hoenderop JGJ. Active Ca(2+) reabsorption in the connecting tubule. Pflugers Arch. 2009; 458(1):99–109. https://doi.org/10.1007/s00424-008-0602-6 PMID: 18989697.

100. van Goor MKC, Hoenderop JGJ, van der Wijst J. TRP channels in calcium homeostasis: from hormonal control to structure-function relationship of TRPV5 and TRPV6. Biochim Biophys Acta Mol Cell Res. 2017; 1864(6):883–93. https://doi.org/10.1016/j.bbamcr.2016.11.027 PMID: 27913205.

101. Jou-Valencia D, Molema G, Popa E, Aslan A, van Dijk F, Mencke R, et al. Renal Klotho is Reduced in Septic Patients and Pretreatment With Recombinant Klotho Attenuates Organ Injury in Lipopolysaccharide-Challenged Mice. Crit Care Med. 2018; 46(12):e1196–e1203. https://doi.org/10.1097/CCM.0000000000003427 PMID: 30239382.

102. Kamr AM, Dembek KA, Hildreth BE, Morresey PR, Rathgeber RA, Burns TA, et al. The FGF-23/klotho axis and its relationship with phosphorus, calcium, vitamin D, PTH, aldosterone, severity of disease, and outcome in hospitalised foals. Equine Vet J. 2018; 50(6):739–46. https://doi.org/10.1111/evj.12946 PMID: 29660161.

103. Ohyama Y, Kurabayashi M, Masuda H, Nakamura T, Aihara Y, Kaname T, et al. Molecular Cloning of RatklothocDNA: Markedly Decreased Expression ofklothoby Acute Inflammatory Stress. Biochem Biophys Res Commun. 1998; 251(3):920–5. https://doi.org/10.1006/bbrc.1998.9576 PMID: 9791011

104. Cóndor JM, Rodrigues CE, Sousa Moreira Rd, Canale D, Volpini RA, Shimizu MHM, et al. Treatment With Human Wharton's Jelly-Derived Mesenchymal Stem Cells Attenuates Sepsis-Induced Kidney Injury, Liver Injury, and Endothelial Dysfunction. Stem Cells Transl Med. 2016; 5(8):1048–57. https://doi.org/10.5966/sctm.2015-0138 PMID: 27280799.

105. Bi F, Chen F, Li Y, Wei A, Cao W. Klotho preservation by Rhein promotes toll-like receptor 4 proteolysis and attenuates lipopolysaccharide-induced acute kidney injury. J Mol Med. 2018; 96(9):915–27. https://doi.org/10.1007/s00109-018-1644-7 PMID: 29730698.

106. Chen X, Tong H, Chen Y, Chen C, Ye J, Mo Q, et al. Klotho ameliorates sepsis-induced acute kidney injury but is irrelevant to autophagy. Onco Targets Ther. 2018; 11:867–81. https://doi.org/10.2147/OTT.S156891 PMID: 29497318.

107. Jorge LB, Coelho FO, Sanches TR, Malheiros DMAC, Ezaquiel de Souza L, Dos Santos F, et al. Klotho deficiency aggravates sepsis-related multiple organ dysfunction. Am J Physiol Renal Physiol. 2019; 316(3):F438–F448. https://doi.org/10.1152/ajprenal.00625.2017 PMID: 30516423.

108. Yan F, Feng Y, Chen J, Yan J. Klotho downregulation contributes to myocardial damage of cardiorenal syndrome in sepsis. Mol Med Rep. 2020; 22(2):1035–43. https://doi.org/10.3892/mmr.2020.11178 PMID: 32468073.

109. Dai B, David V, Martin A, Huang J, Li H, Jiao Y, et al. A comparative transcriptome analysis identifying FGF23 regulated genes in the kidney of a mouse CKD model. PLoS ONE. 2012; 7(9):e44161. https://doi.org/10.1371/journal.pone.0044161 PMID: 22970174.

110. Fitzpatrick EA, Han X, Xiao Z, Quarles LD. Role of Fibroblast Growth Factor-23 in Innate Immune Responses. Front Endocrinol (Lausanne). 2018; 9:320. https://doi.org/10.3389/fendo.2018.00320 PMID: 29946298.

111. David V, Francis C, Babitt JL. Ironing out the cross talk between FGF23 and inflammation. Am J Physiol Renal Physiol. 2017; 312(1):F1–F8. https://doi.org/10.1152/ajprenal.00359.2016 PMID: 27582104.